

Supporting Information

Ultrasoft Silicon Nanomembranes: Thickness-dependent Effective Elastic Modulus

Ajit K. Katiyar^{†*}, Ashwini Ann Davidson^{†*}, Houk Jang[†], Yun Hwangbo[‡], Byeori Han[†], Seonwoo Lee[†], Yohei Hagiwara[§], Takahiro Shimada^{§**}, Hiroyuki Hirakata[§], Takayuki Kitamura[§] and Jong-Hyun Ahn^{†**}

[†]School of Electrical and Electronic Engineering, Yonsei University, 50 Yonsei-ro, Seoul 03722, Republic of Korea

[‡]Department of Nano Mechanics, Nano Convergence and Manufacturing Systems Research Division, Korea Institute of Machinery & Materials (KIMM), 156 Gajeongbuk-ro, Daejeon 34103, Republic of Korea

[§]Department of Mechanical Engineering and Science, Kyoto University, Nishikyo-ku, Kyoto 615-8540, Japan

*These authors (Katiyar A. K. and Davidson A. A.) contributed equally to this work

**Corresponding Author: ahnj@yonsei.ac.kr and shimada@me.kyoto-u.ac.jp

S1. Membrane and thin-plate theory

The applied strain in top and bottom faces of the membrane under bending/stretching can be estimated based on the membrane theory.^{11,12} The overall membrane dynamics is governed via the ratio a/h , where “ a ” is the width of the membrane and “ h ” is the thickness, and is applicable for ratio values above 80. For a ratio <8 , the system is considered as a thick plate, whereas for a ratio of 8–80, it is considered as a thin plate. Along with above mentioned dimensional criteria, few other experimental conditions need to be met to treat the system as a membrane. The first criterion is that the membrane should be free from any transverse shear forces and moments. The second criterion is that the membrane should be structurally uniform and have minimum lattice defects. All the investigated Si NM samples can be fully considered as membranes and not plates. The main criterion of the a/h ratio is fully satisfied for the used dimensions of each thickness. For the second criterion, our starting material was single crystalline Si on top of the SOI wafers, which is supposed to have negligible lattice defects.

S2. Theoretical modeling of Young’s modulus for Si nanomembranes

We performed first-principles density-functional theory (DFT) calculations using the projector-augmented wave (PAW) method as implemented in the Vienna *ab initio* simulation package (VASP) code. The electronic wave functions were expanded in plane wave up to a kinetic energy of 350 eV. The gradient-corrected exchange-correlation functional proposed by Perdew, Burke, and Ernzerhof (PBE) was employed.

Si NMs were modeled using the slab super cell geometry including the vacuum thickness of 2 nm, which was sufficient to neglect the undesirable interaction from the neighboring slabs. The x , y , and z directions of the Si NM model were taken to the [011], [0-11], and [100] axes of the Si diamond crystal lattice. The (100) surface was allowed to relax to the p(2x1) reconstruction. We prepared the Si NMs with different thickness ranging from 0.8-4 nm. The $6 \times 10 \times 1$ Monkhorst-Pack k -point sampling was used for the Brillouin zone integration. To evaluate the Young’s modulus, a small increment of tensile strain was applied along [011] (x) direction. In each straining step, the atomic structure was fully relaxed under the free transverse-stress condition until the Hellmann-Feynman force was reduced below 0.001 eV/Å. The Young’s modulus was calculated from the slope of stress-strain curve obtained from the above straining procedure.

To study the effect of charge concentration due to the formation of surface charge in Si NMs, we also calculated the Young’s modulus with respect to the charge concentration.

We prepared the models with different excess electrons. The homogeneous background charge is imposed to achieve the calculations for the charged model. The strain was applied along [001] direction. The Young's modulus was evaluated in the same manner describe above.

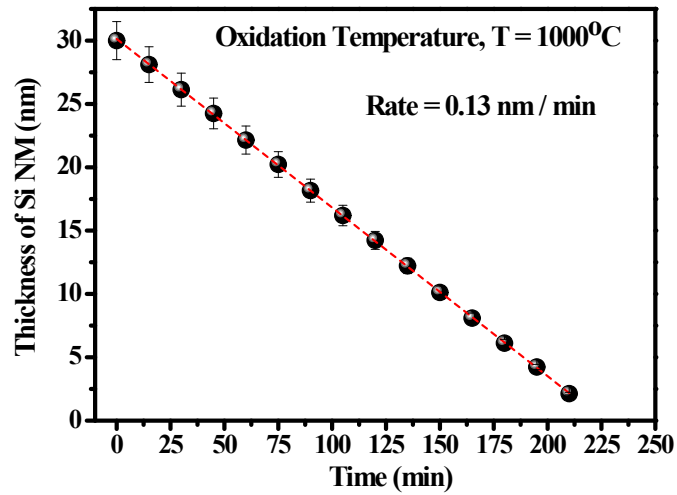


Figure S1. Thickness of Si NMs on SOI wafer as a function of thermal oxidation time. The fitted line shows thermal removal rate of 0.13 nm/min at an oxidation temperature of 1000°C.

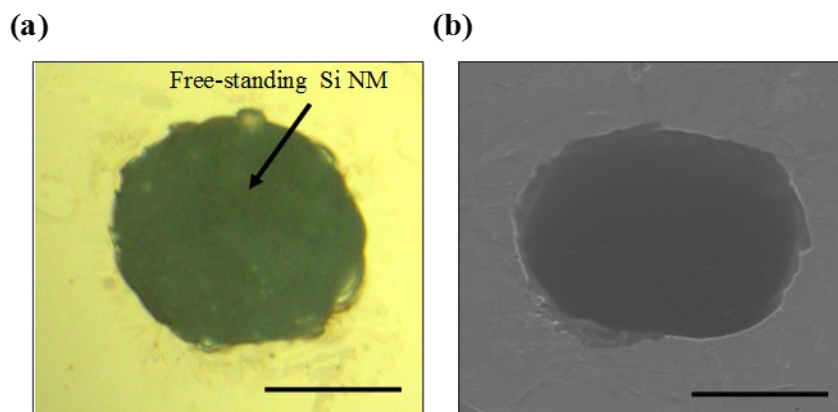


Figure S2. (a) Optical microscopic and (b) SEM images of free-standing 2 nm thick Si nanomembrane suspended on perforated Si substrate (Scale bar: 10 μm in each image).

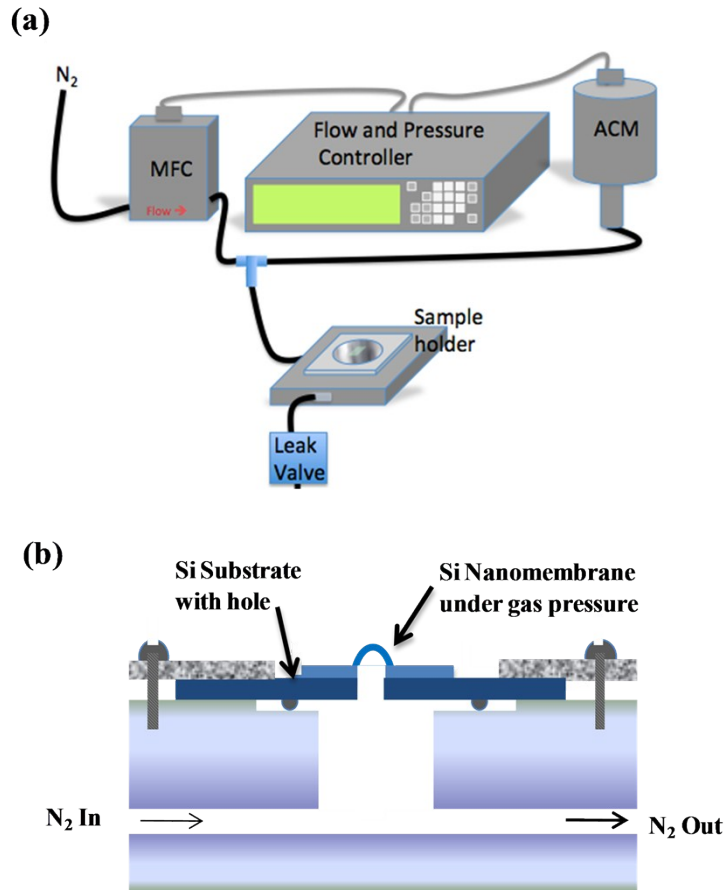


Figure S3. (a) Schematic of bulge tester setup consisting of mass flow controller, absolute capacitance manometer, controller, sample holder, and leak valve. (b) Schematic of the cross-sectional view of the bulge tester sample holder.

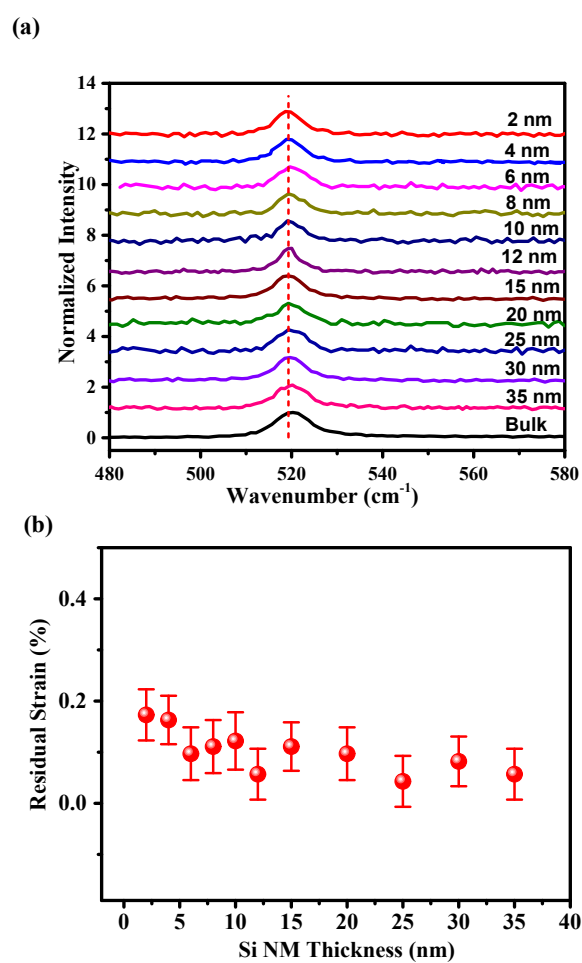


Figure S4. (a) Raman spectra of the suspended membrane samples of different thicknesses without applying gas pressure. (b) Residual strain vs. nanomembrane thickness. Approximately 0.17% of residual strain was observed on the suspended membrane.

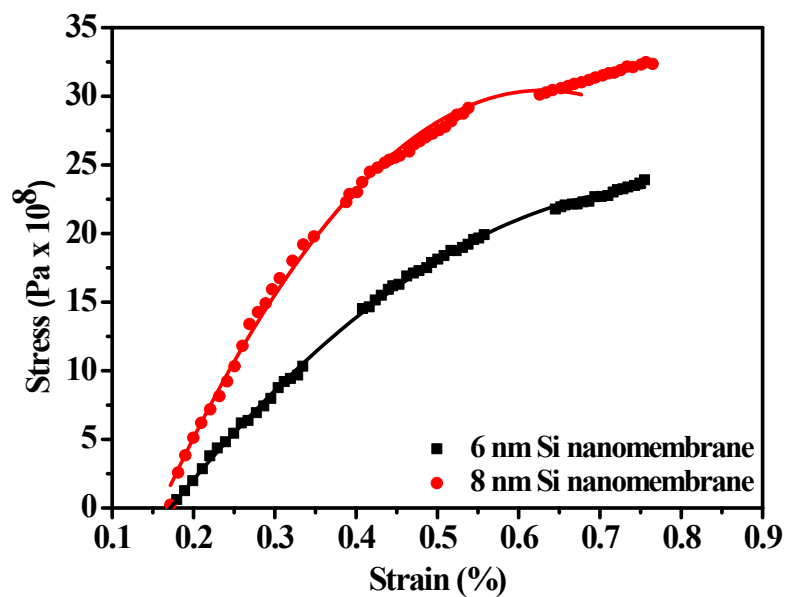


Figure S5. Stress and strain curve of 6 nm and 8 nm Si NM samples when the maximum amount of pressure was applied. The non-linear curves show the beginning of the ductility region.

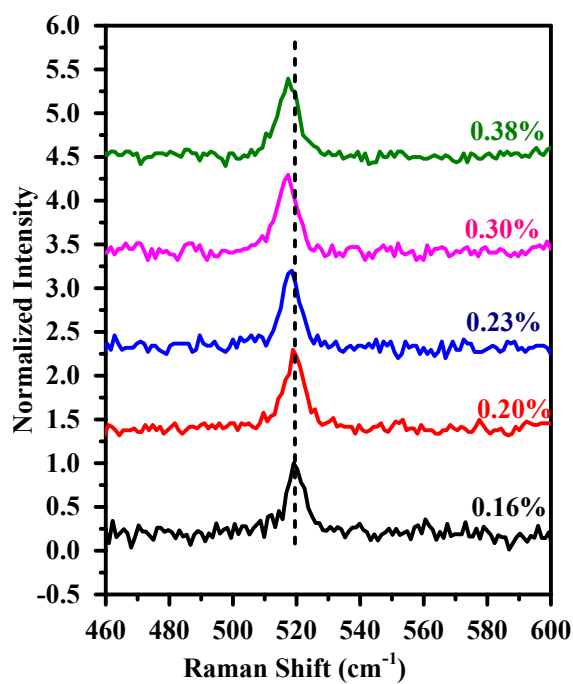


Figure S6. Raman spectra of 10 nm thick Si NM sample recorded during the outward deflection under increasing pressure. (The corresponding height of membrane is shown in Figure 2 (b)).

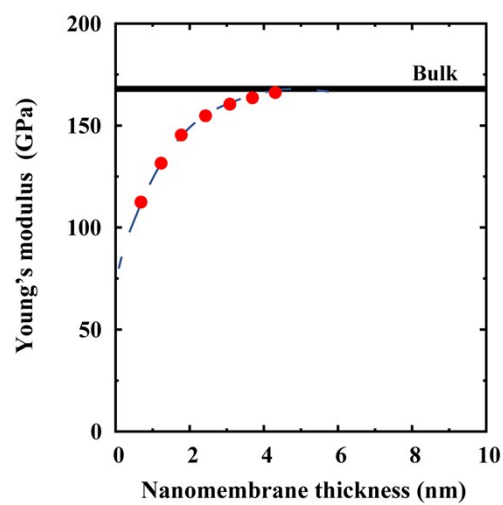


Figure S7. Thickness-dependent Young's modulus of pristine Si (100) NMs obtained from first-principles calculations.

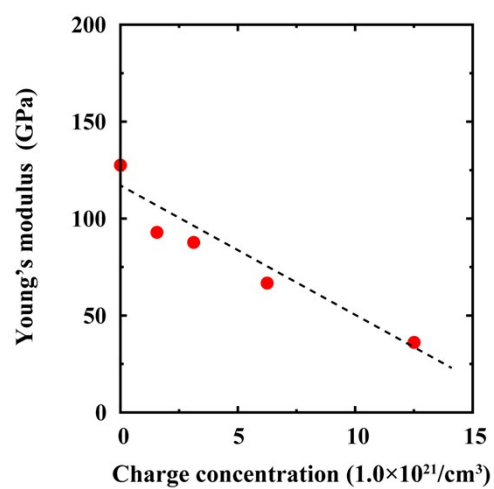


Figure S8. Young's modulus of silicon as a function of charge concentration obtained from first-principles calculations.